Original Paper

Cells Tissues Organs

Cells Tissues Organs 2011;193:135–150
DOI: 10.1159/000319970

Accepted after revision: June 15, 2010
Published online: September 28, 2010

Analysis of the Presence of Cell Proliferation-Related Molecules in the *Tgf-β3* Null Mutant Mouse Palate Reveals Misexpression of EGF and *Msx-1*

A. del Río[a] M.C. Barrio[a] J. Murillo[a] E. Maldonado[a] Y. López-Gordillo[a]
E. Martínez-Sanz[a] M.L. Martínez[b] C. Martínez-Álvarez[a]

[a]Departamento de Anatomía y Embriología Humana I, Facultad de Odontología, Universidad Complutense de Madrid, y [b]Departamento de Física Aplicada y Óptica/Sección de Óptica, Facultad de Farmacia, Universidad San Pablo, CEU, Madrid, España

Key Words
Tgf-β3 · Knockout · Palate · Epidermal growth factor · *Msx-1*

Abstract
The *Tgf-β3* null mutant mouse palate presents several cellular anomalies that lead to the appearance of cleft palate. One of them concerns the cell proliferation of both the palatal medial edge epithelium and mesenchyme. In this work, our aim was to determine whether there was any variation in the presence/distribution of several cell proliferation-related molecules that could be responsible for the cell proliferation defects observed in these palates. Our results showed no difference in the presence of EGF-R, PDGF-A, TGF-β_2, *Bmp-2*, and *Bmp-4*, and differences were minimal for FGF-10 and *Shh*. However, the expression of EGF and *Msx-1* changed substantially. The shift of the EGF protein expression was the one that most correlated with that of cell proliferation. This molecule is regulated by TGF-β_3, and experiments blocking its activity in culture suggest that EGF misexpression in the *Tgf-β3* null mutant mouse palate plays a role in the cell proliferation defect observed.

Abbreviations used in this paper

AP	Anterior-posterior
Bmp-2	Bone morphogenetic protein 2
Bmp-4	Bone morphogenetic protein 4
BrdU	5-bromo-2′-deoxy-uridine
CP	Cleft palate
DMEM/F12	Dulbecco's modified Eagle's medium/ Ham's F12 growth medium
E	Embryonic day
EGF	Epidermal growth factor
EGF-R	Epidermal growth factor receptor
FGF-10	Fibroblast growth factor 10
MEE	Medial edge epithelium
MES	Midline epithelial seam
Msx-1	msh homeobox 1
PBS/DEPC	Phosphate buffered saline/diethylopyrocarbonate
PDGF-A	Platelet-derived growth factor A
PFA	Paraformaldehyde
Shh	Sonic hedgehog
TGF-β_2	Transforming growth factor-β_2
TGF-β_3	Transforming growth factor-β_3
Tgf-β3 –/–	*Tgf-β3* null mutant mouse
WT	Wild type

KARGER

Fax +41 61 306 12 34
E-Mail karger@karger.ch
www.karger.com

1422–6405/11/1933–0135$38.00/0

Accessible online at:
www.karger.com/cto

Dr. Concepción Martínez-Álvarez
Departamento de Anatomía y Embriología Humana I
Facultad de Odontología, Universidad Complutense de Madrid
Avda. Complutense, s/n, ES–28040 Madrid (Spain)
Tel. +34 91 394 1905, Fax +34 91 394 1910, E-Mail cmartinez@med.ucm.es

Introduction

In mammals, formation of the secondary palate includes the growth, development, and fusion of 2 palatal shelves that arise from the medial aspect of the maxillary processes of the first branchial arch. In the mouse, as a result of mesenchymal cell proliferation [Burdett et al., 1988], palatal shelves appear in the oropharynx on embryonic day 11.5 (E11.5). They then grow downwards at both sides of the tongue until E14, and in the subsequent 12 h they rotate on an anterior-posterior (AP) axis, allowing their tips to face each other. At E14.5, the epithelia covering these tips [medial edge epithelium (MEE)] make contact with one another [Ferguson, 1988]. Opposing MEE cells adhere strongly by means of cell adhesion and cell matrix molecules [Martínez-Álvarez et al., 2000a; Gato et al., 2002; Tudela et al., 2002; Martínez-Sanz et al., 2008], intercalate [Tudela et al., 2002], and form the midline epithelial seam (MES). The MES cells disappear soon after by undergoing cell death [Mori et al., 1994; Martínez-Álvarez et al., 2000b; Cuervo and Covarrubias, 2004; Takigawa and Shiota, 2004; Vaziri Sani et al., 2005], epithelial-to-mesenchymal transformation [Fitchett and Hay, 1989; Shuler et al., 1992; Martínez-Álvarez et al., 2000b; Jin and Ding, 2006], and migration [Carette and Ferguson, 1992; Cuervo and Covarrubias, 2004; Jin and Ding, 2006]. By E15.5 in the mouse, the palate is completely fused.

The *Tgf-β_3* null mutant mouse (*Tgf-β_3* –/–) palatal shelves do not fuse properly. They grow, rotate, and come into contact in the midline, but their opposing MEE either do not adhere at all, resulting in a complete cleft of the secondary palate, or do so poorly, leading to the appearance of an incomplete cleft palate (CP) [Kaartinen et al., 1995; Proetzel et al., 1995; Taya et al., 1999, Gato et al., 2002, Resel et al., 2007]. This altered palatal shelf adhesion is due to the abnormal presence of chondroitin sulphate proteoglycan, fibronectin, and the α5-integrin in the *Tgf-β_3* –/– mouse MEE, which are crucial for palatal shelf adhesion [Gato et al., 2002; Martínez-Sanz et al., 2008]. At this time point (E14.5), a decreased cell proliferation has been observed in the *Tgf-β_3* –/– mouse palatal mesenchyme [Xu et al., 2006], which could impede either good or prolonged contact between palatal shelves, thus reducing the opportunities for an already compromised palatal shelf adhesion. In fact, a CP develops when palatal mesenchymal cell proliferation is low [Rice et al., 2004; Yu et al., 2005]. Finally, in those areas of the *Tgf-β_3* –/– mouse palate where palatal shelf adhesion has succeeded and an MES has formed, increased MEE cell proliferation [Cui et al., 2003], decreased MES cell death [Martínez-Álvarez et al., 2000a; Yang and Kaartinen, 2007], and impaired epithelial-to-mesenchymal transformation and migration [Kaartinen et al., 1997; Nawshad et al., 2007] prevent MES disintegration, thus causing the failure of palatal fusion (mesenchymal confluence).

We and others have reported the misexpression of several growth and transcription factors in the *Tgf-β_3* –/– mouse palate which cause some of these alterations [Martínez-Álvarez et al., 2004; Knight et al., 2006; Sasaki et al., 2007; Murillo et al., 2009]. In the present work, we hypothesized that the presence of 1 or more molecules related to cell proliferation has shifted in the *Tgf-β_3* –/– mouse palate and that this is responsible for the change in cell proliferation. We analyzed the distribution pattern of epidermal growth factor (EGF), EGF-receptor (EGF-R), FGF-10, platelet-derived growth factor (PDGF)-A, transforming growth factor (TGF)-β_2, *Msx-1*, *Bmp-2, Bmp-4*, and *Shh* in the wild type (WT) and *Tgf-β_3* –/– mouse palate at the time when palatal shelves first make contact, which is the critical time for palatal shelf adhesion. Both EGF and EGF-R were immunolocalized in the MEE and mesenchyme at all stages of palate development [Shiota et al., 1990; Dixon et al., 1991; Citterio and Gaillard, 1994; Jaskoll et al., 1996]. EGF has a recognized mitogenic activity in the MEE and mesenchyme of the developing palate [Abbott and Pratt, 1988; Gawel-Thompson and Greene, 1989; Yamamoto et al., 2003], while EGF-R –/– mice exhibit CP and delayed palatal shelf closure [Miettinen et al., 1999]. Furthermore, alterations of the EGF signaling pathway have been claimed to be the ultimate cause of some teratogenically induced CP [Abbott and Pratt, 1987; Bryant et al., 2001; Abbott et al., 2005]. The *Fgf-10* transcripts are observed from E11.5 to E13.5 in the anterior part of the palate [Alappat et al., 2005]. PDGF is a ubiquitous mitogen which predominantly stimulates the proliferation of connective tissue cells [Heldin and Westermark, 1990]. Although the *Pdgf-a* –/– mice that survive do not bear a CP [Betsholtz et al., 2001], the presence of PDGF-A has been described in the palate at all developmental stages [Qiu et al., 1995]. TGF-β_2 is observed in the WT mouse palatal mesenchyme prior to and during palatal fusion [Fitzpatrick et al., 1990], where it has been seen to inhibit cell proliferation [Nugent et al., 1998]. Zhang et al. [2002] investigated the presence of *Msx-1*, *Bmp-2, Bmp-4*, and *Shh* in the palatal MEE and mesenchyme of E11–13 WT mouse palates. The presence of some of these molecules had been previously detected in the developing palate [Bitgood and McMahon, 1995; Turecková et al., 1995; Nugent and Greene, 1998; Lu et al.,

2000], but the main interest of the work of these researchers was to find orchestrated interactions between them which stimulated mesenchymal cell proliferation. In fact, all of these molecules are important to palatal development since either null mutations or the overexpression of all of these genes or their receptors results in CP [Satokata and Maas, 1994; Liu et al., 2005; Cobourne et al., 2009; Meng et al., 2009].

Our study shows the presence of some of these molecules in parts of the E14.5 WT palate in which they were not present at earlier stages. We also show that in the *Tgf-β3* –/– palate the most altered molecules are EGF and *Msx-1*. The EGF protein expression shift observed in these palates greatly correlates with that of cell proliferation, which is reduced when the EGF-R activity is inhibited in culture.

Animals and Methods

Animals

The C57/BL/6J WT and *Tgf-β3* heterozygous mice (Jackson Laboratories, Bar Harbor, Me., USA) were mated. The day of vaginal plug detection was designated as day 0. Time-mated pregnant mice were killed by an overdose of chloroform. The embryos were removed by median laparotomy, placed in cold 1/1 Dulbecco's modified Eagle's medium/Ham's F12 growth medium (DMEM/F12; Sigma-Aldrich, Inc., St. Louis, Mo., USA) supplemented with 1% penicillin/streptomycin, and decapitated. The embryos to be used for culture experiments were removed under sterile conditions. Once the heads were obtained the jaws and tongues were removed. Genotyping was performed as described by Martínez-Álvarez et al. [2000b]. The animal facilities and the experimental protocol used in the studies reported herein were reviewed and approved by the Experimental Animal Committee of the Universidad Complutense de Madrid.

Palatal Shelf Organ Cultures

Under sterile conditions, E14 WT and *Tgf-β3* –/– mouse palatal shelves were microsurgically extracted, placed isolated on a 2 × 2 mm Millipore filter with a 0.8-μm pore size (Millipore Corp., Bedford, Mass., USA), and cultured in Trowell's tissue culture in DMEM/F12 supplemented with 2% penicillin/streptomycin and 1% ascorbic acid at 37°C in a 5% CO_2 incubator. The agents added to these cultures were 10 ng/ml recombinant human (rh) TGF-β_3 (R&D Systems, Inc., Minneapolis, Minn., USA) or 100 μM tyrphostin AG1478 (Sigma-Aldrich). The cultures were only incubated for 12 h since longer culture periods have shown MEE disappearance [Takigawa and Shiota, 2004].

Cell Proliferation Detection

In order to detect cell proliferation in the embryonic heads and cultures, a 5-bromo-2′-deoxy-uridine (BrdU) kit (Roche Diagnostics Corp., Indianapolis, Ind., USA) was used. Briefly, 1 h prior to embryo extraction, 2 ml/100 g body weight BrdU was injected into the pregnant female intraperitoneally. The embryos for this study were extracted at E13.5, E14.5, and E16.5. The E14.5 embryos were chosen among those having both elevated and proximal, but not adhered, palatal shelves (fig. 1A). Subsequently, 100 μl of BrdU was placed over each palatal shelf culture 1 h prior to fixation and then reincubated. Embryos and cultures were fixed in Carnoy's fixative for 2 and 1 h, respectively, and embedded in paraffin. Immunohistochemistry with the anti-BrdU antibody from the kit was then performed on 5-μm thick sections. Nitroblue tetrazolium/5-bromo-4-chloro-3-indolyl-phosphate (Roche) was used as a substrate to visualize the sites of BrdU incorporation.

Assessment of Cell Proliferation

BrdU-positive cells in sections from E13.5, E14.5, and E16.5 WT (n = 4 in all cases) and *Tgf-β3* –/– (n = 4 in all cases) mouse heads or WT and *Tgf-β3* –/– mouse palatal shelf cultures, which were untreated or treated with tyrphostin (n = 4 for each genotype and treatment), were measured. The number of sections measured in each experimental condition was between 135 and 205. For in vivo experiments, sections from the anterior and posterior parts of the palate were taken as indicated in figure 1A. Sections from palatal shelf cultures were taken from the posterior half.

Once the image was captured using a MetaMorph image analyzer (version 7.01; Universal Imaging Corp., Sunnyvale, Calif., USA), a fixed area of either the MEE or mesenchyme was selected. The way these areas were obtained is shown in figure 1B (for E13.5 and E14.5 in vivo palatal shelves) and figure 1C (for palatal shelf cultures), which were drawn manually using the MetaMorph image analyzer (fig. 1D, E). A 300-μm-long line (a–b) was drawn in the palatal shelf coronal axis, starting immediately below the MEE. A line (c–d) perpendicular to a–b was then drawn from the oral to the nasal side of the palatal shelf. The area of mesenchyme underneath the palatal epithelia delimited laterally by this line (c–d) was the area of mesenchyme taken for measurement. To determine the MEE area, the bisector of the 2 angles between lines a–b and c–d was obtained (lines a–e and a–f). The area of MEE between the 2 bisectors was the one considered for measurement. Since E16.5 WT palates do not have MEE, only the mesenchyme was considered for cell proliferation measurement in E16.5 WT and *Tgf-β3* –/– mouse samples. Cell proliferation in the mesenchyme of the E16.5 *Tgf-β3* –/– mouse palates (presenting a complete CP) was measured as previously described. To compare the cell proliferation obtained in the mesenchyme of these palates with that from the WT mice of the same stage, the area of mesenchyme taken in the *Tgf-β3* –/– palate was transported to the mesenchyme adjacent to the midline in the WT, where complete palatal fusion had occurred.

Once the areas were determined, the observer fixed the threshold color of the BrdU-positive cells, and the MetaMorph counted the number of spots having the color range selected. The measures for each group are the median values of the number of BrdU-positive cells from all sections of the group. Sections from the control and each experimental condition were measured in the same session to avoid differences in the basal parameters.

Statistical Analysis

For cell proliferation analysis the results are presented as means ± confidence interval (95%). ANOVA and Student's t tests were used to compare normal groups from each experimental condition. $p < 0.01$ or $p < 0.05$ was considered statistically significant.

Immunohistochemistry

The E14.5 WT and *Tgf-β_3* –/– mouse heads were fixed overnight in buffered formaldehyde. The TGF-β_3 or tyrphostin AG1478 treated or untreated WT and *Tgf-β_3* –/– palatal shelf cultures were fixed in paraformaldehyde (PFA) for 2 h. Standard paraffin embedding was then performed and 5-μm sections were obtained. For anti-PDGF-A, anti-FGF-10, and anti-TGF-β_2, the epitope was unmasked using 1 mM EDTA (Sigma-Aldrich). Sections were then incubated for 2 h at room temperature with either 15 μg/ml (for mouse heads) or 5 μg/ml (for cultures) polyclonal goat IgG anti-mouse EGF (R&D Systems), 1:15 polyclonal rabbit IgG anti-human EGF-R (Santa Cruz Biotechnology, Inc., Santa Cruz, Calif., USA), 1:100 polyclonal goat IgG anti-human PDGF-A (Santa Cruz Biotechnology), 1:50 polyclonal goat IgG anti-human FGF-10 (Santa Cruz Biotechnology) or 1:75 polyclonal rabbit IgG anti-human TGF-β_2 (Santa Cruz Biotechnology). Incubation with these antibodies was followed by the addition of a biotinylated anti-goat IgG secondary antibody (Vector Laboratories, Ltd., Peterborough, UK) and an ABC Kit (Pierce Chemical Company, Rockford, Ill., USA) for EGF, PDGF-A, and FGF-10, a goat anti-rabbit IgG horseradish peroxidase conjugated secondary antibody (Chemicon International, Inc., Temecula, Calif., USA) for EGF-R, and a Rabbit/Mouse EnVision™ Peroxidase System (Dako, Carpinteria, Calif., USA) for TGF-β_2 labeling. Negative controls were performed using mouse or rabbit IgG (Santa Cruz Biotechnology) at the same concentrations and conditions used for the respective experimental studies. Some sections were counterstained with hematoxylin for a few seconds prior to mounting. Labeling in sections was visualized using a Leica DMRB microscope and photographed using a Leica DFC320 digital camera (Leica Geosystems AG, St. Gallen, Switzerland). No fewer than 4 different specimens per antibody and experimental condition were analyzed.

In situ Hybridization

The *Msx-1*, *Bmp-2, Bmp-4*, and *Shh* probes were kindly provided by Professor F. Unda of the Universidad del País Vasco, Spain. The E14.5 WT and *Tgf-β_3* –/– mouse heads were extracted in ice-cold PBS/DEPC and fixed overnight in 4% PFA in PBS/DEPC. Once the mouse heads had been fixed, all mandibles, cranial vaults, and encephala were removed. Three different experiments for each experimental condition on no fewer than 4 samples were performed. A 613-bp fragment of murine *Msx-1* cDNA subcloned into PCRII+(AmpR) was digested with BamHI (New England BioLabs, Inc., Ipswich, Mass. USA) and transcribed with T7 RNA polymerase (Roche) for the antisense probe. Fragments of murine *Shh* cDNA (642 bp), *Bmp-2* cDNA (797 bp), and *Bmp-4* cDNA (953 bp) subcloned into pBS-SK+(AmpR) were digested with HindIII (New England BioLabs), Eco 52I (Takara Bio, Inc., Japan), and EcoRI (New England BioLabs), respectively. The *Shh* fragment was transcribed with T3 RNA polymerase (Roche), while *Bmp-2* and *Bmp-4* were transcribed with SP6 (Roche) for the antisense probe. Whole-mount in situ hybridization was performed as described by Martínez-Álvarez et al. [2004]. After hybridization, the heads were incubated with an alkaline phosphatase-conjugated antidigoxigenin antibody. Samples from each experimental condition were developed simultaneously, visualized with a Nikon SMZ800 dissecting microscope (Nikon Corp., Tokyo, Japan), and photographed simultaneously with a fully manually-operated digital Nikon Coolpix 995 camera (Nikon). They were then embedded in gelatin, sectioned with a Leica VT 1000M vibratome, and stored in PBS containing 50% glycerol. The sections were studied using a Leica DMR microscope and photographed with a Leica DFC320 digital camera.

Results

Cell Proliferation Is Altered All Along the Tgf-β_3 –/– *Developing Palate at the Time of the Contact between Palatal Shelves*

E14.5 *Tgf-β_3* –/– mice have been shown to present an altered pattern of cell proliferation in both the palatal MEE [Cui et al., 2003] and the mesenchyme [Xu et al., 2006]. However, a discriminative analysis of that proliferation in the anterior and posterior parts of this mouse palate has never been conducted. This is important since, in WT mice from earlier stages, some molecules have been reported to act differently on cell proliferation depending on the palatal region considered [Hilliard et al., 2005]. Therefore, we measured the presence of BrdU-positive cells in both the anterior and posterior parts of the E14.5 WT and *Tgf-β_3* –/– palatal MEE and mesenchyme. MEE and palatal mesenchyme cell proliferation showed an increased gradient from the anterior part to the posterior part (fig. 2A–F) in both genotypes. Compared to the WT, the E14.5 *Tgf-β_3* –/– mouse MEE showed a significantly augmented number of proliferating cells in both the anterior ($p < 0.05$) and posterior ($p < 0.01$) parts of the palate (fig. 2A–E). However, cell proliferation clearly decreased in this mouse palatal mesenchyme, especially in the posterior region (fig. 2A–D, F).

To determine whether the changes observed in the cell proliferation of *Tgf-β_3* –/– mouse palates at E14.5 also occurred earlier or later than the critical time of contact between palatal shelves, we compared cell proliferation in samples from E13.5 and E16.5 WT and *Tgf-β_3* –/– mouse palates. As observed in E14.5 palates, E13.5 mouse palates showed a statistically higher cell proliferation rate in the posterior part of the palatal mesenchyme than in the anterior part, but no differences were observed between the 2 genotypes (fig. 2G, H). Very low cell proliferation was observed in the palatal mesenchyme of both genotypes at E16.5, with no differences appreciated between them (not shown).

Therefore, the precontacting WT and *Tgf-β_3* –/– mouse palatal shelves show a gradient of increased cell proliferation from the anterior part to the posterior part. Compared to the WT, the *Tgf-β_3* –/– mouse palate has increased MEE and decreased mesenchymal cell prolif-

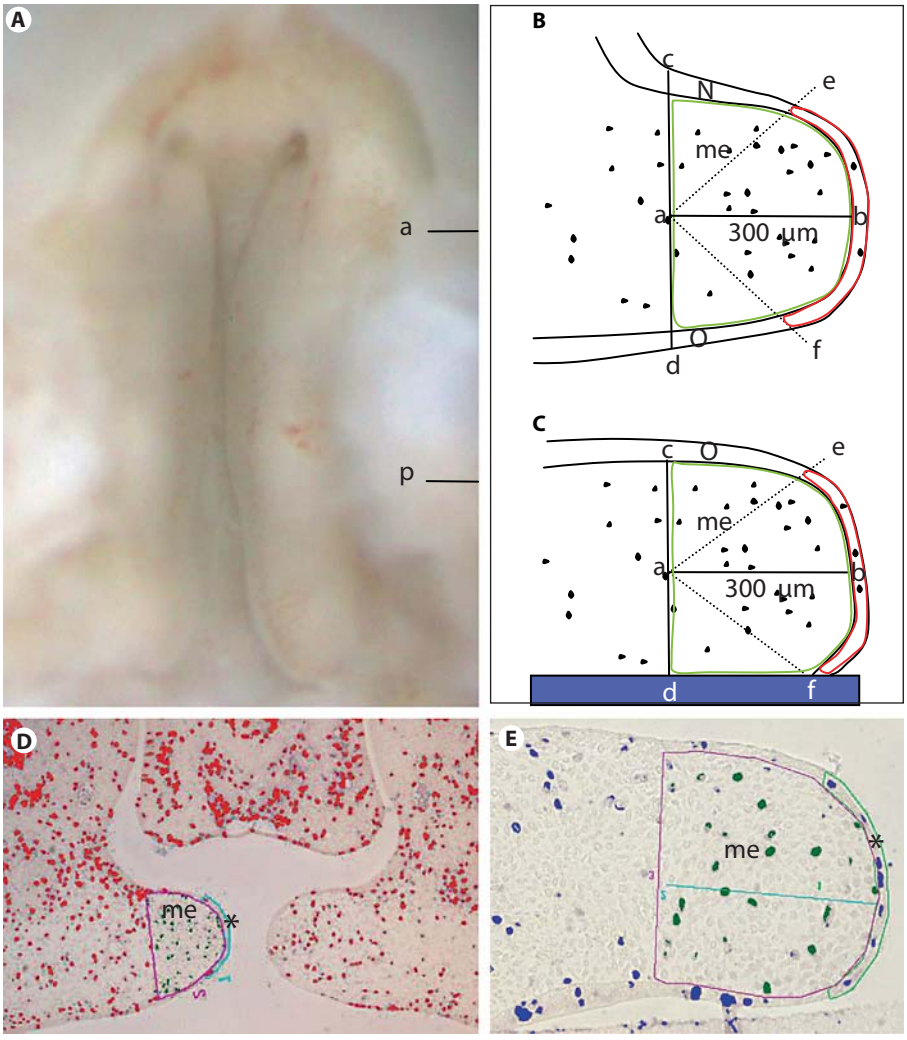

Fig. 1. Measurement of cell proliferation in the mouse embryonic palate in vivo and in vitro. **A** Intraoral view of an E14.5 mouse palate showing almost contacting palatal shelves. The lines indicate the anterior (a) and posterior (p) levels from where the anterior and posterior sections were selected. **B**, **C** Method used to determine the area of MEE and mesenchyme for counting BrdU-labeled cells in vivo (**B**) and in vitro (**C**). The area of mesenchyme and MEE taken for measurement is surrounded by a green and a red line, respectively. Line a–b is placed in the coronal axis of the palatal shelf and is 300 μm long. Line c–d is perpendicular to line a–b and goes from the oral (O) to the nasal (N) palatal epithelium. Lines a–e and a–f are the bisectors of the angles formed by lines a–b and c–d. **D**, **E** Images as captured by the MetaMorph image analyzer with the areas of MEE and palatal mesenchyme selected for measurement. * = MEE; me = palatal mesenchyme.

eration at the critical time of contact between palatal shelves (E14.5), showing no differences at earlier or later stages.

The Presence of EGF, but Not of EGF-R, FGF-10, PDGF-A, or TGF-β_2, Is Altered in the E14.5 Tgf-β_3 –/– Palate

The presence of a cell proliferation shift all along the palate in the E14.5 *Tgf-β_3* –/– mouse embryo made us wonder whether any of the molecules present in the developing palate, having been correlated with the induction/inhibition of cell proliferation, were altered at this stage. We analyzed the presence of EGF, EGF-R, FGF-10, PDGF-A, and TGF-β_2 (fig. 3) using immunohistochemistry.

EGF labeling was intracellular in the WT and *Tgf-β_3* –/– MEE and mesenchyme (fig. 3A–D). Its presence was evident in both halves of the palate, although it was more marked in the posterior half (fig. 3A, B). Compared to the WT, the *Tgf-β_3* –/– palate had a much greater marked anti-EGF labeling in the MEE, but it was reduced in the mesenchyme. This shift was especially evident in the posterior half of the palate (compare fig. 3C, D with 3A, B).

EGF-R labeling was also intracellular in both the WT and *Tgf-β_3* –/– mouse palates (fig. 3E–H). Its presence was scarce in both the palatal MEE and mesenchyme of the whole palate. No differences were observed in the presence of this protein between the WT and *Tgf-β_3* –/– (fig. 3E–H) palates.

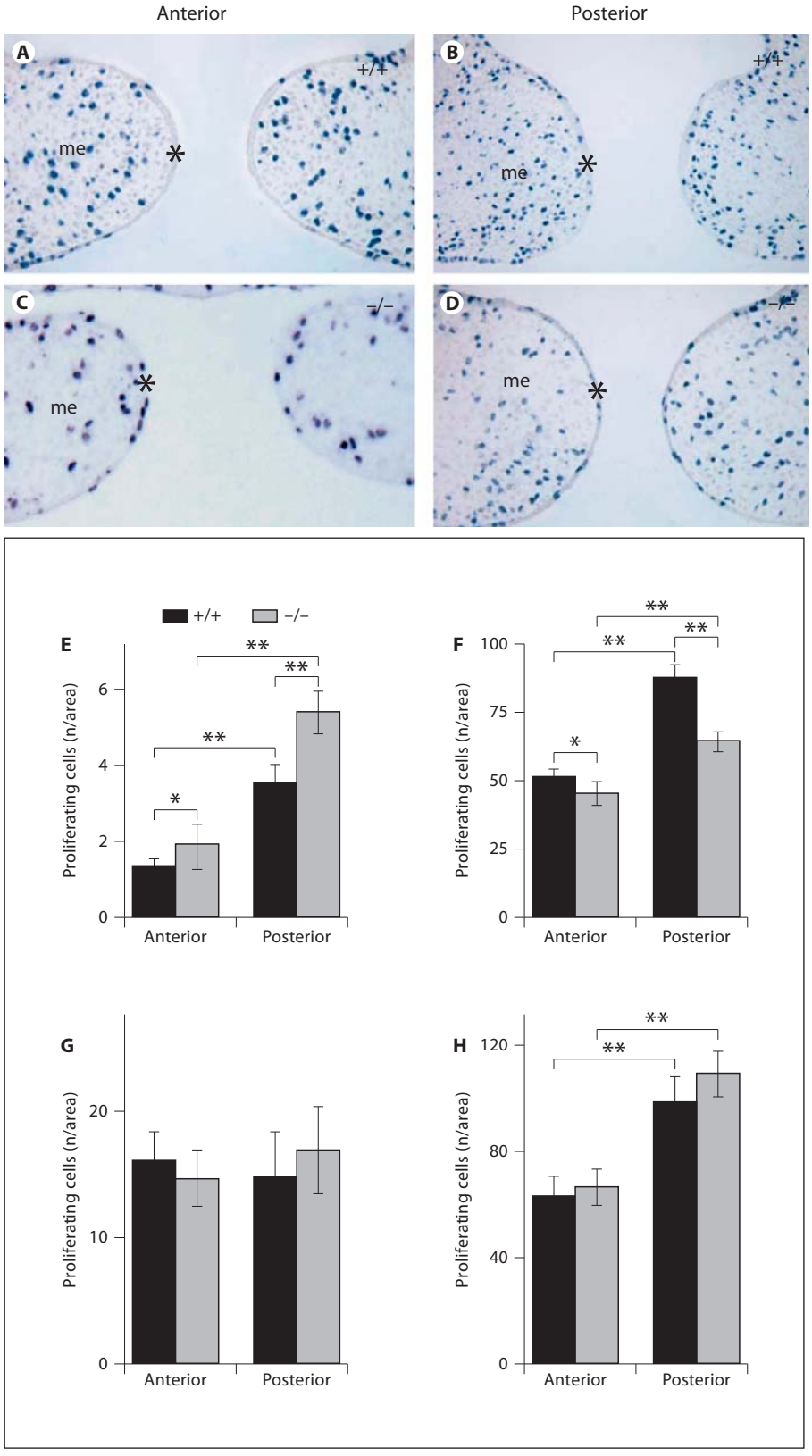

Fig. 2. Presence of BrdU-labeled cells in the WT and *Tgf-β3* null embryonic palates. **A–D** Sections from WT (**A**, **B**) and *Tgf-β3* null (**C**, **D**) mouse palates taken from the anterior (**A**, **C**) and posterior (**B**, **D**) parts of the palates. The asterisks represent the MEE. **E–H** Comparison of the mean values of cell proliferation in MEE (**E**, **G**) and mesenchyme (**F**, **H**) E14.5 (**E**, **F**) and E13.5 (**G**, **H**) WT and *Tgf-β3* –/– mouse palates. Notice the AP increasing gradient of cell proliferation in both the WT and *Tgf-β3* –/– palates, as well as the significant increase in cell proliferation in the MEE (**E**) and the decrease in the mesenchyme (**F**) of the mutant at E14.5. No difference in cell proliferation is observed between the 2 genotypes at E13.5 (**G**, **H**). * $p < 0.05$; ** $p < 0.01$. me = Palatal mesenchyme.

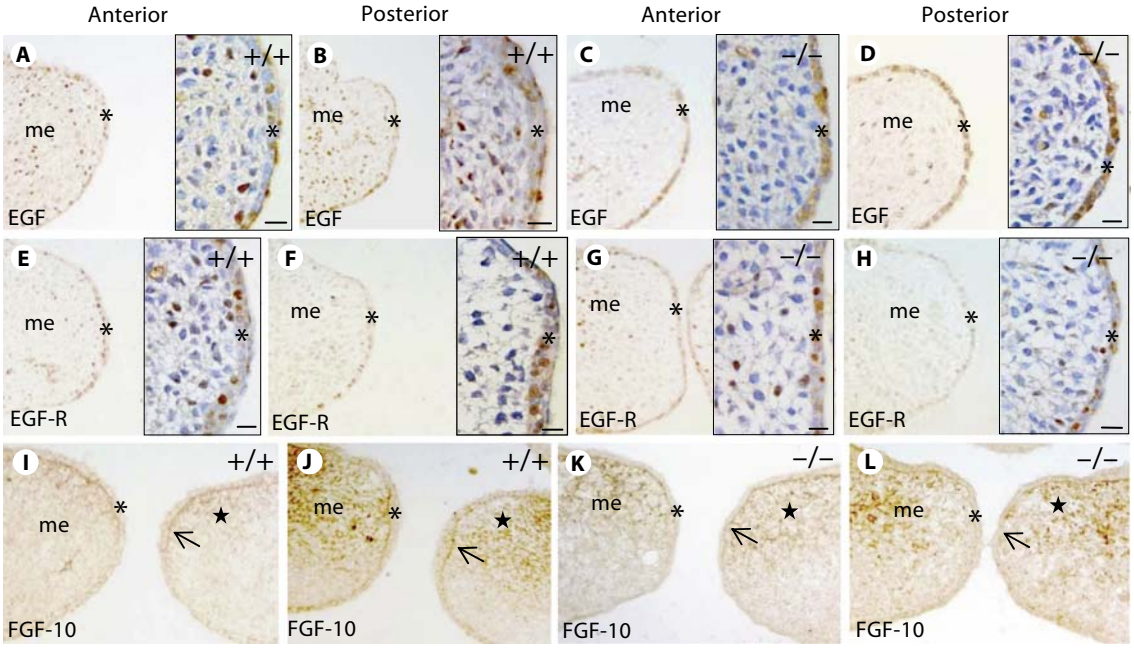

Fig. 3. Immunolocalization of EGF (**A–D**), EGF-R (**E–H**), and FGF-10 (**I–L**) in the WT (**A**, **B**, **E**, **F**, **I**, **J**) and *Tgf-β3* null (**C**, **D**, **G**, **H**, **K**, **L**) embryonic palates. Sections were taken from the anterior (**A**, **C**, **E**, **G**, **I**, **K**,) and posterior (**B**, **D**, **F**, **H**, **J**, **L**) parts of the palates. Notice the difference between the WT and *Tgf-β3* –/– mouse palates in the presence of EGF in the MEE and mesenchyme and in the presence of FGF-10 in the basement membrane (arrow in **I–L**). FGF-10 labeling is observed on the nasal (star in **I–L**) but not on the oral side of the palatal shelves. **A–H** Insets correspond to hematoxylin-eosin counterstained sections from the samples. * = MEE; me = palatal mesenchyme. Scale bar = 10 μm.

FGF-10 was extracellular, present in the palatal mesenchyme, and absent in the MEE of WT and *Tgf-β3* –/– palates (fig. 3I–L). Labeling in the mesenchyme also seemed to have an increased gradient from the anterior part to the posterior part. The basement membrane was strongly labeled in the WT palate (fig. 3I, J) but practically unlabelled in that of the *Tgf-β3* –/– (fig. 3K, L). In both WT and mutants, the nasal half of the palate was more markedly labeled than the oral half.

PDGF-A and TGF-β_2 showed a similar pattern of labeling and distribution in the WT and *Tgf-β3* –/– palates without presenting regional differences (not shown).

In summary, these results revealed a striking difference in the presence of EGF in the palates from WT and *Tgf-β3* –/– mice, with only a minimal variation in FGF-10 labeling and no differences in the presence of EGF-R, PDGF-A, or TGF-β_2.

Expression of Msx-1, but Not of Bmp-2, Bmp-4, or Shh, Is Altered in the Tgf-β_3 *–/– Palate*

Zhang et al. [2002] described the expression of *Msx-1, Bmp-2, Bmp-4*, and *Shh* in the palates from E11–13.5 WT mice and reported a hierarchy among them for inducing mesenchymal cell proliferation. We thus analyzed the expression of all of these molecules in the *Tgf-β3* –/– and WT mouse palates (fig. 4–7). As reported for E13.5 [Zhang et al., 2002], the E14.5 WT mouse palatal shelves only showed *Msx-1* expression in the mesenchyme of their anterior half (fig. 4A–C), which was absent in the MEE (fig. 4B, C). The expression in the mesenchyme followed a clear gradient from the anterior part to the posterior part and from the medial part to the lateral part (fig. 4A–C). This gradient was absent in the *Tgf-β3* –/– palate (fig. 4D–F). There was no *Msx-1* expression in the *Tgf-β3* –/– MEE (fig. 4E, F) either.

The expression of *Bmp-2* and *Bmp-4* was similar in E14.5 WT and *Tgf-β3* –/– mouse palates (fig. 5, 6) and only visible in the mesenchyme (fig. 5B, C, E, F, 6B, C, E, F). The expression of *Bmp-2* was strong in the most medial palatal mesenchyme of the anterior region (fig. 5A, B, D, E) but less marked in the posterior part (fig. 5A, C, D, F). The expression of *Bmp-4* was marked in the mesenchyme immediately underlying the medial side of the first 2 rugae (fig. 6A, B, D, E) and more diffuse in the rest

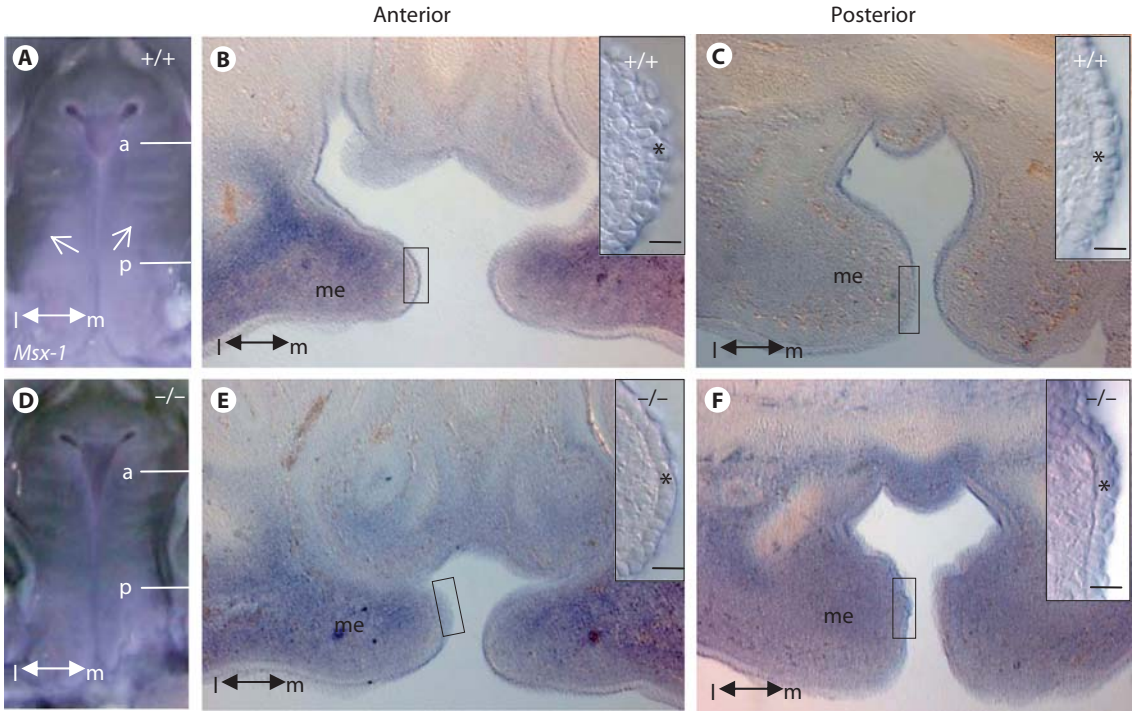

Fig. 4. Presence of *Msx-1* transcripts in the WT (**A–C**) and *Tgf-β3* null (**D–F**) embryonic palates. **A**, **D** Representation of an intraoral view of these palates. **B–F** Sections taken from their anterior (**B**, **E**) and posterior (**C**, **F**) parts. Lines in **A**, **D** represent the level of anterior (a) and posterior (p) parts of the palate where the sections in **B–F** were taken. The lateral and medial parts of the palate are indicated by l–m. **B–F** Insets are high-power magnifications of the boxed areas. Notice the AP and medial-lateral loss of *Msx-1* expression in the WT palate (arrows in **A**), which is not present in the *Tgf-β3* null mutant, and the presence of *Msx-1* transcripts in the posterior part of the palate in the *Tgf-β3* null mutant (**F**), which are not present in the WT (**C**). There is no *Msx-1* expression in the MEE from either genotypes (asterisks in the insets in **B**, **C**, **E**, **F**). me = Palatal mesenchyme. Scale bar = 10 μm.

of the mesenchyme. The mesenchyme of the posterior half of the palate presented remarkable *Bmp-4* expression (fig. 6A, C, D, F).

A comparison of *Shh* expression between WT and *Tgf-β3* –/– mouse palates has already been reported [Sasaki et al., 2007]. Contrary to what was observed by these researchers, we found very little difference in *Shh* expression between these palates (fig. 7). As previously described for the WT secondary palate [Sasaki et al., 2007, Pantalacci et al., 2008], high *Shh* expression was observed in the epithelium of the rugae and on the oral side of the future soft palate of both genotypes (fig. 7). The only difference found between them was the *Shh* expression observed in the medial part of the first ruga, which extended more medially in the WT than in the *Tgf-β3* –/– palate (fig. 7A, B, D, E).

Therefore, little or no variation exists in the expression of *Bmp-2, Bmp-4,* and *Shh* between the WT and *Tgf-β3* –/– mouse palates, whereas there is an abnormal distribution of *Msx-1*.

In vitro Addition of TGF-β3 to Tgf-β3 *–/– Palatal Shelves Rescues the Normal EGF Protein Expression Pattern*

To demonstrate the influence of TGF-β3 on the presence of EGF in the palate, we cultured palatal shelves from E14 *Tgf-β3* –/– mice in the presence or absence of TGF-β3. After the incubation period, these palatal cultures were immunolabeled with an antibody directed against EGF (fig. 8A–C). As expected, immunolabeling of WT and untreated *Tgf-β3* –/– palatal cultures with anti-EGF showed a pattern of EGF expression similar to the one observed in vivo (compare fig. 8A, B with fig. 3A–D). Treatment of *Tgf-β3* –/– palatal cultures with TGF-β3 resulted in a reduced presence of EGF in the MEE when compared with their untreated counterparts (compare

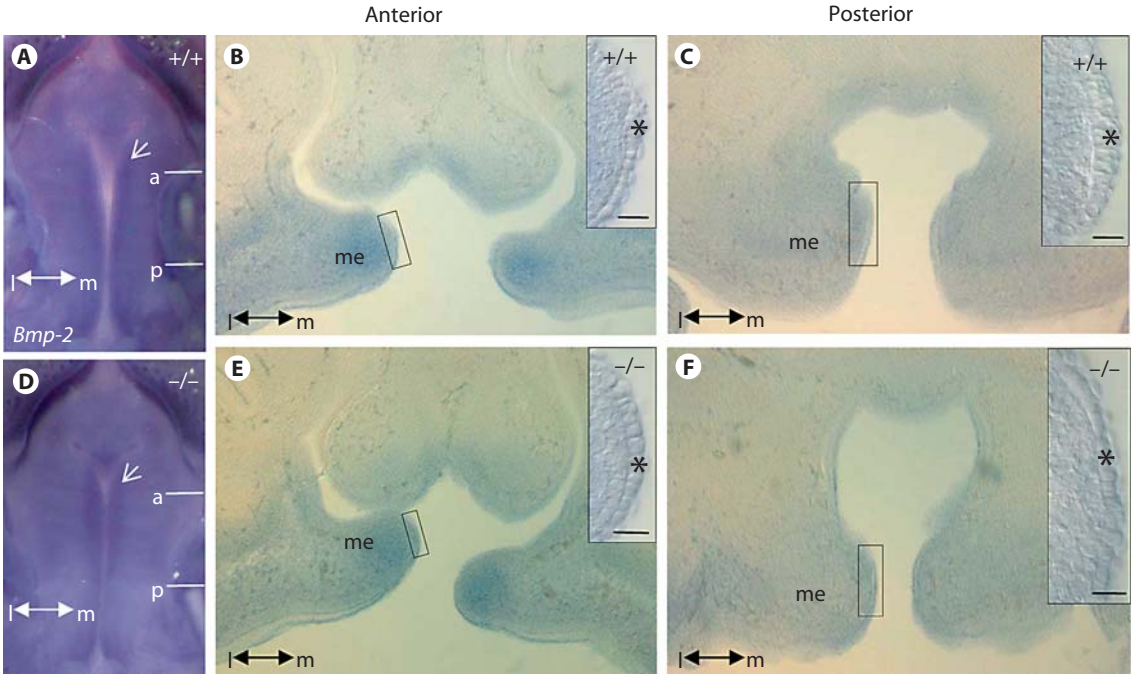

Fig. 5. *Bmp-2* expression in the WT (**A–C**) and *Tgf-β3* null (**D–F**) embryonic palates. **A**, **D** Intraoral views of these palates. **B–F** Sections taken from their anterior (**B**, **E**) and posterior (**C**, **F**) parts. Lines in (**A**, **D**) represent the level of anterior (a) and posterior (p) parts of the palate where the sections in **B–F** were taken. The lateral and medial parts of the palatal shelves are indicated by l–m. **B–F** Insets are high-power magnifications of the squared areas. There is a strong *Bmp-2* expression in the mesenchyme of the anterior region (arrow in **A**, **D**; **B**, **E**) which is weaker in the posterior part (**C**, **F**). Notice the absence of *Bmp-2* expression in the MEE (asterisks in the insets in **B**, **C**, **E**, **F**). No differences are noticeable between the 2 genotypes. me = Palatal mesenchyme. Scale bars = 10 μm.

fig. 8C with B), thereby showing a pattern similar to cultured WT palates (compare fig. 8C with A).

We thus demonstrated that the EGF presence in the MEE is under the influence of TGF-β_3.

In vitro Inhibition of EGF-R Activity Reduces Cell Proliferation in the WT and Tgf-β_3 *–/– Palate and Causes Increased EGF Protein Expression*

To determine whether there is participation of EGF in the altered cell proliferation observed in the *Tgf-β3* –/– palates, we inhibited EGF-R activity in culture by adding tyrphostin AG1478, a tyrosine kinase inhibitor specifically selective for EGF-R [Abud et al., 2005], to the culture medium of the left *Tgf-β3* –/– palatal shelves. An equal amount of PBS was added to the right ones. The experiment was also carried out with WT palatal shelves. Less cell proliferation was observed in vitro than in vivo for WT and *Tgf-β3* –/– palatal MEE and mesenchyme, although the proportions between the 2 genotypes were maintained (compare fig. 8D, E with fig. 2E, F). A comparison of the number of BrdU-labeled cells present in both MEE and palatal mesenchyme between tyrphostin-treated and untreated *Tgf-β3* –/– palatal shelves revealed a significant decrease ($p < 0.01$) in proliferating cells when EGF-R activity was inhibited (fig. 8D, E). In the WT tyrphostin-treated cultures, the MEE but not the mesenchyme showed a significant reduction in cell proliferation.

To further analyze whether tyrphostin AG1478 was really inhibiting the EGF-R, we immunolabeled WT and *Tgf-β3* –/– mouse palatal shelf cultures, untreated or treated with tyrphostin AG1478, with an anti-EGF antibody. Compared to WT controls (fig. 8F), WT tyrphostin-treated cultures showed a clear increase in EGF protein expression in the mesenchyme (fig. 8G). This increase was much less evident in the *Tgf-β3* –/– cultures (compare fig. 8H and I).

This demonstrates that the abnormal presence of EGF has a role in the cell proliferation alteration observed in the *Tgf-β3* –/– developing palate.

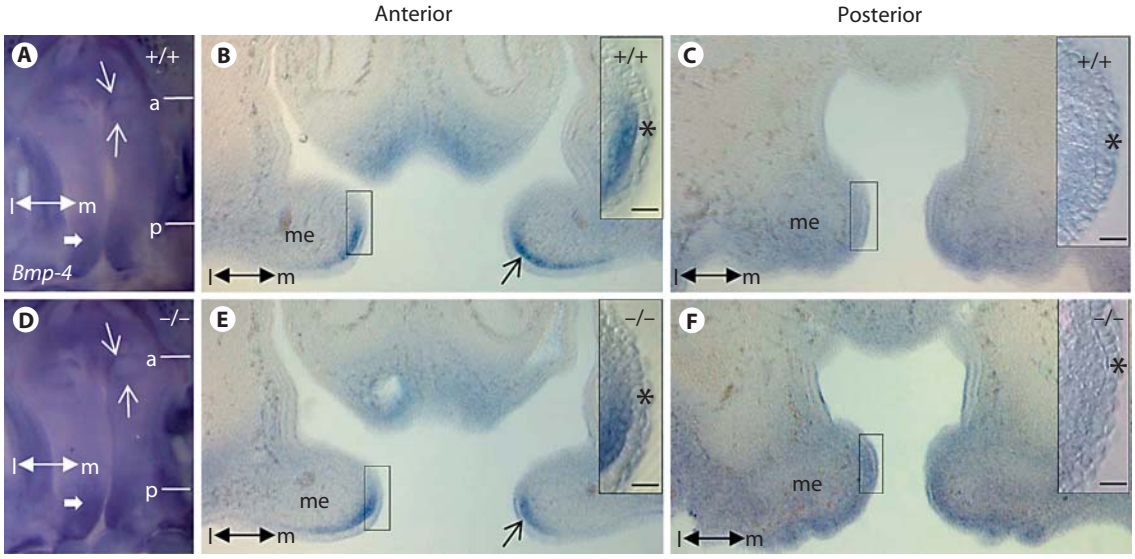

Fig. 6. Presence of *Bmp-4* transcripts in the WT (**A–C**) and *Tgf-β3* null (**D–F**) embryonic palates. **A**, **D** Intraoral views of these palates, with the sections in **B–F** taken from their anterior (**B**, **E**) and posterior (**C**, **F**) parts. The anterior (a) and posterior (p) parts of the palate where the sections in **B–F** were taken are indicated in **A**, **D**. The lateral and medial parts of the palatal shelves are indicated by l–m. **B–F** Insets are high-power magnifications of the boxed areas. There is a strong *Bmp-4* expression in the mesenchyme underlying the 2 first rugae (arrows in **A**, **B**, **D**, **E**) and in the mesenchyme of the posterior part of the palate (thick arrow in **A**, **D**; **C**, **F**). Notice the absence of *Bmp-4* expression in the MEE (asterisks in the insets in **B**, **C**, **E**, **F**). No differences are evident between the 2 genotypes. me = Palatal mesenchyme. Scale bar = 10 μm.

Discussion

In this work, we analyzed the presence and distribution of several cell proliferation-related molecules in the developing palate of *Tgf-β3* –/– mice and correlated the changes observed with those occurring in cell proliferation.

First, our analysis of the presence of cell proliferation in the E13.5 and E14.5 WT palate revealed the existence of an increasing AP gradient of cell proliferation. This gradient of cell proliferation was reported at early stages of palate development [Shah et al., 1994, Rice et al., 2004] and, since DNA synthesis decreases as the palate develops [Hudson and Shapiro, 1973; Pratt and Martin, 1975; Greene and Pratt, 1976], it is an exponent of the known AP gradient of differentiation occurring during palatal development [Hilliard et al., 2005]. The increasing AP gradient of cell proliferation was maintained in the *Tgf-β3* –/– palate, thus indicating that the AP differentiation pattern is not lost in these mice. However, cell proliferation rates were substantially different in both the MEE and mesenchyme with respect to the WT at the time of contact between palatal shelves. In the *Tgf-β3* –/– MEE, the amount of proliferating cells increased significantly in both the anterior and posterior parts of the palate. This confirms the results obtained by Cui et al. [2003], although these authors did not distinguish between palatal regions. On the contrary, in the *Tgf-β3* –/– palatal mesenchyme, cell proliferation strikingly decreased with respect to the WT. The existence of a significant decrease in cell proliferation in the *Tgf-β3* –/– palatal mesenchyme has already been reported [Xu et al. 2006]. Our demonstration here that this occurs all along the palate reinforces these previous results. Interestingly, cell proliferation was not altered in the *Tgf-β3* –/– palates earlier during development, thus explaining why *Tgf-β3* –/– palatal shelves grow properly towards their contact in the midline. The cell proliferation rate was not different between the 2 genotypes when palatal shelf fusion was completed in the WT (E.16.5). The *Tgf-β3* gene is expressed in the mouse palate between E13 and E15 [Fitzpatrick et al., 1990; Pelton et al., 1990]. The fact that cell proliferation is only significantly altered in the *Tgf-β3* –/– palate immediately prior to the contact between palatal shelves suggests that the absence of TGF-β_3 alters palatal cell proliferation indirectly through the possibly unbalanced presence of other molecules having a role in this mechanism.

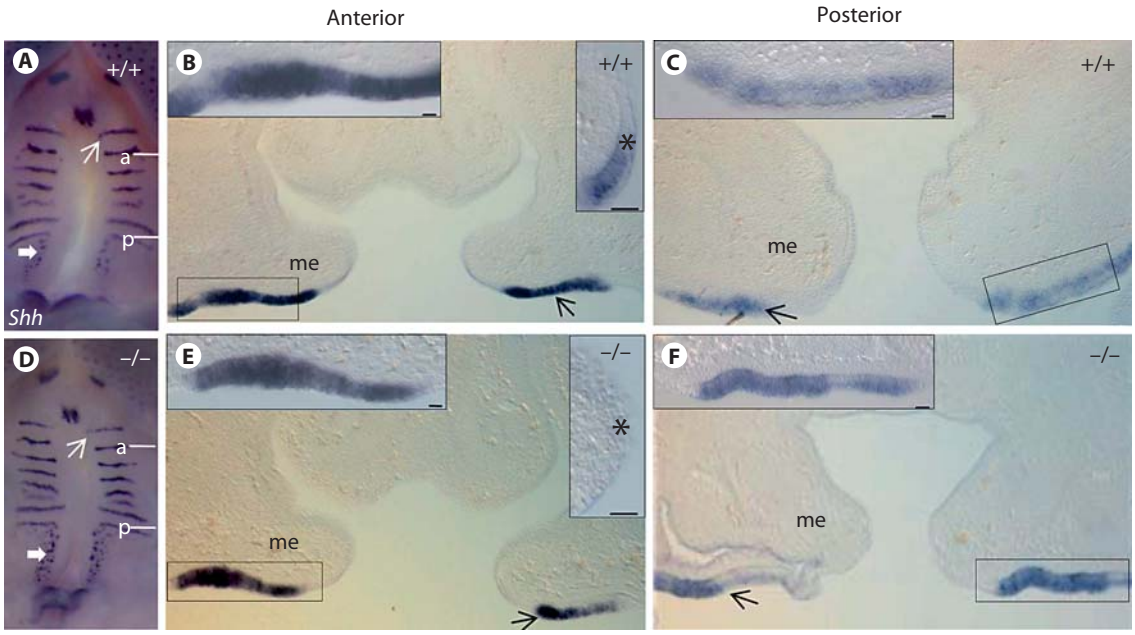

Fig. 7. *Shh* expression in the WT (**A–C**) and *Tgf-β3* null (**D–F**) embryonic palates. **A**, **D** Intraoral view of these palates. **B–F** Sections taken from their anterior (**B**, **E**) and posterior (**C**, **F**) parts. The anterior (a) and posterior (p) parts of the palate where the sections in (**B–F**) were taken are labeled in (**A**, **D**). **B–F** Insets in the left corner are high-power magnifications of the boxed areas. **B**, **E** Insets in the right corner were taken at the level of the first ruga. Observe the presence of *Shh* transcripts in the epithelium of the palatal rugae (thin arrow in **B–F**) and the salivary glands in the soft palate (thick arrow in **A**, **D**). The *Shh* transcripts extend medially in the WT palate (thin arrow in **A** and inset in the right corner of **B**) but not in the *Tgf-β3* null mutant (thin arrow in **D** and inset in the right corner of **E**). * = MEE; me = palatal mesenchyme. Scale bar = 10 μm.

We did not find *Msx-1* transcripts in the mesenchyme from the posterior part of the E14.5 WT palate. This is congruent with the results obtained at the same stage by Levi et al. [2006] and reveals that the regionalization pattern of *Msx-1* expression in the palate does not vary during development. This also suggests that *Msx-1* does not have any influence on the high cell proliferation rate observed in the posterior part of the palate at this stage, as it does during earlier stages of development [Zhang et al., 2002]. The EGF and EGF-R protein expression levels observed in this study did not show any difference compared with expression levels reported previously [Dixon et al., 1991] although, to the best of our knowledge, differences in EGF labeling between the anterior and posterior parts of the palate have never been described. These differences correlated well with the cell proliferation distribution observed along the palate, as reported for the facial primordia at earlier stages [Iamaroon et al., 1996]. Very little expression of *Fgf-10* has been reported to be present at E14 in the WT mouse [Rice et al., 2004], and this expression has been reported only on the oral side of the palate. However, we found expression of the FGF-10 protein on the nasal side of the palatal mesenchyme, thus coinciding with the described expression of its receptor *Fgfr2* [Rice et al., 2004; Hilliard et al., 2005], which suggests that the FGF-10 activity is mainly exerted on this side of the palate. There is no previously reported data on the regionalization of FGF-10 on the AP axis of the palate at E14.5. Up to E13.5, *Fgf-10* expression has only been observed in the anterior part of the palate [Rice et al., 2004; Alappat et al., 2005], but at E14.5 we found a stronger expression of the FGF-10 protein in the posterior region than in the anterior region. Together with the presence of *Bmp-2* and *Bmp-4* in this part of the palate at this stage [Lu et al., 2000; Nie, 2005; this work], this important expression of FGF-10 could also account for the increased proliferation rate observed in the posterior part of the palate at this time point.

Little difference in the expression of most of the analyzed molecules was observed in the E14.5 *Tgf-β3* –/– mouse palate compared to the WT. In fact, no difference was noticed for EGF-R, PDGF-A, TGF-β_2, *Bmp-2*, and *Bmp-4*, and the difference was minimal for FGF-10 and *Shh*. Although the amount and distribution of FGF-10 in

Fig. 8. Rescue of the EGF expression pattern in TGF-β_3 treated *Tgf-β_3* null palatal shelf cultures and consequences of EGF-R inhibition on cell proliferation and EGF protein expression in WT and *Tgf-β_3* null palatal shelf cultures. WT (**A**) and *Tgf-β_3* null (**B**, **C**) palatal shelf cultures untreated (**A**, **B**) or treated (**C**) with 10 ng/ml TGF-β_3 and immunolabeled with an anti-EGF antibody. Notice the strong anti-EGF labeling in the *Tgf-β_3* null MEE of the untreated cultures (**B**) and the weak labeling in the treated ones (**C**), considering the aspect observed in the WT (**A**). Measurement of cell proliferation in the MEE (**D**) or mesenchyme (**E**) of WT and *Tgf-β_3* null palatal shelf cultures treated with PBS (control) or tyrphostin. Compared to the controls, all treated cultures show a significant (** $p < 0.01$) reduction in cell proliferation, except for the mesenchyme of the treated WT palatal shelf cultures. **F–I** Immunolabeling with anti-EGF of WT (**F**, **G**) and *Tgf-β_3 –/–* (**H**, **I**) palatal shelf cultures untreated (**F**, **H**) or treated (**G**, **I**) with tyrphostin AG1478. Observe the strong anti-EGF labeling in the mesenchyme of the WT treated cultures (**G**). * = MEE; me = palatal mesenchyme; S = TGF-β_3 supplemented; Tyr = tyrphostin treated. Scale bars = 10 μm.

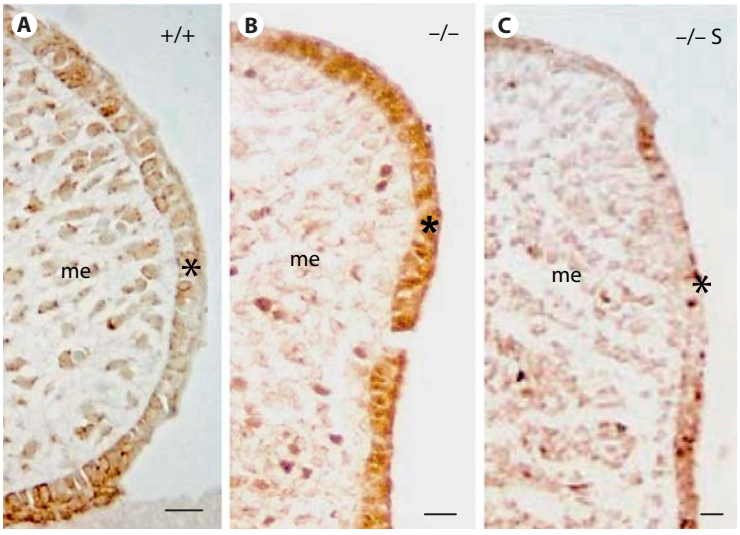

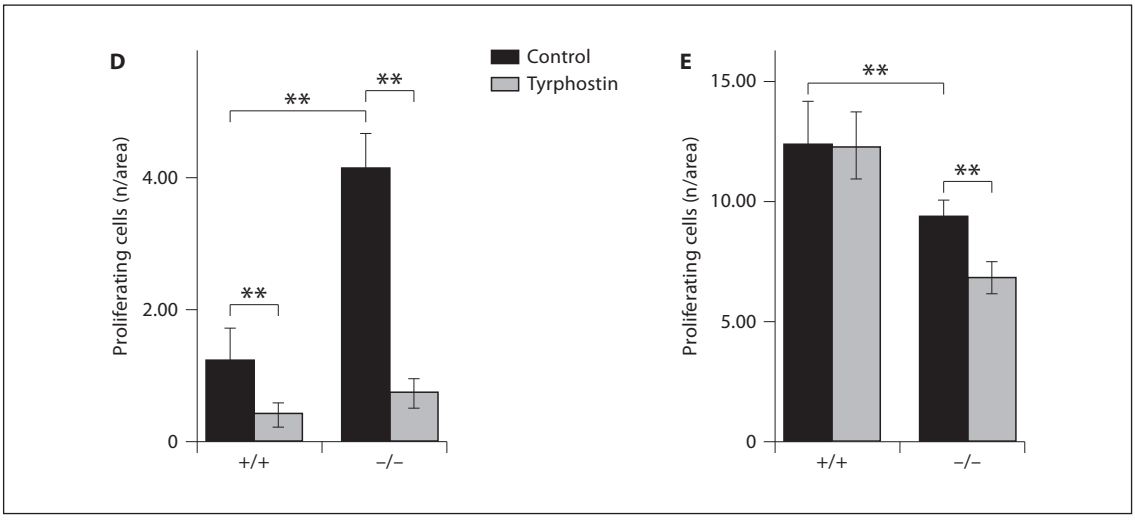

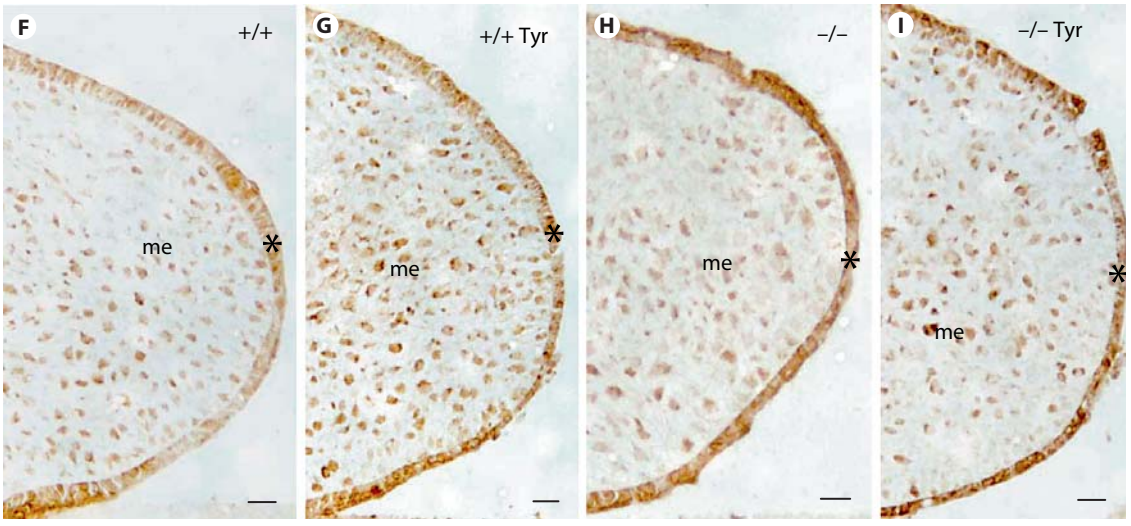

the palatal mesenchyme of *Tgf-β3* –/– was very similar to that found in the WT, its presence in the MEE basement membrane of the mutant was greatly reduced, while strong labeling was observed in the WT. In general, the mesenchyme-produced FGF-10 exerts its effect on epithelia by means of basement membranes [Izvolsky et al., 2003]. The basement membrane is a known reservoir of FGF-10, where it is bound by proteoglycan-containing molecules which allow its gradual release and modulate its activity on, for example, epithelial cell proliferation [Patel et al., 2007]. The absence of retained FGF-10 in the *Tgf-β3* –/– MEE basement membrane could be related to some molecular variations existing at this location in these palates, such as variations in collagen IV, laminin, and certain metalloproteinases [Kaartinen et al., 1997; Blavier et al., 2001; Gato et al., 2002; Martínez-Sanz et al., 2008], which could participate in the alteration of cell proliferation observed in this MEE. Contrary to Sasaki et al. [2007], we did not see a downregulation of *Shh* in the palatal rugae of E14.5 *Tgf-β3* –/– palates. This discrepancy could be related to the different strain of *Tgf-β3* –/– mouse used; the Manchester strain was used in the work by Sasaki and C57/BL6J was used in this work. Indeed, the expression in the developing palate of several other molecules differs between the 2 strains [Martínez-Sanz et al., 2008]. The only change found regarding *Shh* expression in our *Tgf-β3* –/– palates was the lack of medial extension of the expression in the epithelium of the first ruga, which was very clear in the WT. This coincides with the end of the medial growth of the first rugae described in *Tgf-β3* –/– palates which, contrary to those observed in the WT, never make contact at the midline [Taya et al., 1999].

The most striking differences found between the 2 genotypes in the analyzed molecules concerned *Msx-1* and EGF. Whereas in the E14.5 WT palate the area of *Msx-1* expression gradually narrowed from the apex of the palatal shelf mesially to the palatal margin of the molar epithelium distally [Turecková et al., 1995, this work], in the *Tgf-β3* –/– palate this regionalization was lost, and *Msx-1* transcripts were also observed medially in the posterior part of the palate. This demonstrates that, as occurs with TGF-β_1 [Nugent and Greene, 1998], TGF-β_3 modulates *Msx-1* expression in the WT palatal mesenchyme and that this modulation is different in the anterior and posterior parts of the palate. Since TGF-β_3 is present in the MEE of the whole palate, this regionalization might be more related to the known different AP activity of the TGF-β_3 receptor ALK5 [Dudas et al., 2004]. The expression of *Msx-1* has been closely associated with palatal mesenchymal cell proliferation, though restricted to the anterior part of the palate [Barlow et al., 1997; Zhang et al., 2002; Hilliard et al., 2005]. This might be preserved in the *Tgf-β3* –/– mouse palate since the increased *Msx-1* expression observed in its posterior part did not correlate with more cell proliferation. On the contrary, cell proliferation in this part of the mutant palate significantly decreased compared to the WT.

The most altered expression found in the *Tgf-β3* –/– developing palate was the one observed for EGF. Indeed, compared to the WT, in the *Tgf-β3* –/– mouse palate EGF labeling strikingly increased in the MEE and decreased in the mesenchyme, while this shift was reversed, especially in the MEE, when TGF-β_3 was added to *Tgf-β3* –/– palatal shelves in culture. This demonstrates that, as occurs for TGF-β_1 [Sharpe et al., 1992; Brunet et al., 1993; Nugent and Greene, 1998; Weston et al., 1998], TGF-β_3 modulates EGF in the developing palate and, since exogenous EGF has been found to downregulate TGF-β_3 in embryonic palatal tissue [Gehris et al., 1994], it is likely that a cross talk between these 2 molecules is present during palatal development.

The change in EGF protein expression observed at both the MEE and mesenchymal levels in the *Tgf-β3* –/– palate greatly correlated with that observed for cell proliferation, thus suggesting an involvement of EGF in the altered pattern of cell proliferation observed in these palates. This was further confirmed by the significant reduction of cell proliferation in the *Tgf-β3* –/– MEE and palatal mesenchyme when EGF-R activity was inhibited in culture by the EGF-R tyrosine kinase inhibitor AG1478, as seen in this work. Importantly, when the EGF-R activity was blocked in the WT palate, cell proliferation only decreased significantly in the MEE, with the mesenchyme showing no differences compared to the control. EGF protein expression was especially increased in the WT mesenchyme of tyrphostin-treated cultures, probably as an attempt by these cells to compensate for the EGF-R inhibition, which was able to maintain cell proliferation in this tissue. The fact that this did not occur in the WT MEE (where cell proliferation is known to decrease after E13 [Hudson and Shapiro, 1973]) or in the *Tgf-β3* –/– palate provides further evidence of the role of TGF-β_3 in regulating palatal cell proliferation by means of EGF.

In summary, we demonstrated here that the changes in cell proliferation in the *Tgf-β3* null mouse embryonic palate correlate with differences in the presence of some molecules known to have a pivotal role in palatal cell proliferation. Most of those analyzed showed minimal or nonexistent alterations, but the expression of *Msx-1* and

EGF (especially) changed considerably. TGF-β_3 regulates EGF expression, and experiments which block the activity of EGF in palatal shelf cultures suggest that its misexpression in the *Tgf-β_3* null mouse palate causes its cell proliferation defect.

Acknowledgements

The authors wish to thank Ms. Alicia Cerro and Ms. Dolores Arroyo (Universidad Complutense) for their assistance with the histology. We also thank Professor F. Unda (Universidad del País Vasco) for kindly providing the cDNA for the *Msx-1*, *Bmp-2, Bmp-4,* and *Shh* probes, the technical team of the Centro de Microscopía y Citometría of the Universidad Complutense for their assistance with the assessment of cell proliferation, Proof-Reading-Service UK for editing this manuscript for English language, and the anonymous referees for their helpful suggestions in the completion of this manuscript. This work was supported by grants from the Spanish Ministry of Health (PI06/0184 and PS09/01762), the Universidad Complutense-Comunidad Autónoma de Madrid (CCG07-ECM/BIO-2592), and Banco de Santander Central Hispano-Universidad Complutense to the Complutense Research Group (920202) (2008).

References

- Abbott, B.D., D.S. Best, M.G. Narotsky (2005) Teratogenic effects of retinoic acid are modulated in mice lacking expression of epidermal growth factor and transforming growth factor-alpha. Birth Defects Res A Clin Mol Teratol *73:* 204–217.
- Abbott, B.D., R.M. Pratt (1987) Retinoids and epidermal growth factor alter embryonic mouse palatal epithelial and mesenchymal cell differentiation in organ culture. J Craniofac Genet Dev Biol *7:* 219–240.
- Abbott, B.D., R.M. Pratt (1988) EGF receptor expression in the developing tooth is altered by exogenous retinoic acid and EGF. Dev Biol *128:* 300–304.
- Abud, H.E., N. Watson, J.K. Heath (2005) Growth of intestinal epithelium in organ culture is dependent on EGF signalling. Exp Cell Res *303:* 252–262.
- Alappat, S.R., Z. Zhang, K. Suzuki, X. Zhang, H. Liu, R. Jiang, G. Yamada, Y. Chen (2005) The cellular and molecular etiology of the cleft secondary palate in Fgf10 mutant mice. Dev Biol *277:* 102–113.
- Barlow, A.J., P.H. Francis-West (1997) Ectopic application of recombinant BMP-2 and BMP-4 can change patterning of developing chick facial primordia. Development *124:* 391–398.
- Betsholtz, C., L. Karlsson, P. Lindahl (2001) Developmental roles of platelet-derived growth factors. Bioessays *23:* 494–507.
- Bitgood, M.J., A.P. McMahon (1995) Hedgehog and Bmp genes are coexpressed at many diverse sites of cell-cell interaction in the mouse embryo. Dev Biol *172:* 126–138.
- Blavier, L., A. Lazaryev, J. Groffen, N. Heisterkamp, Y.A. DeClerk, V. Kaartinen (2001) TGF-beta3-induced palatogenesis requires matrix metalloproteinases. Mol Biol Cell *12:* 1457–1466.
- Brunet, C.L., P.M. Sharpe, M.W. Ferguson (1993) The distribution of epidermal growth factor binding sites in the developing mouse palate. Int J Dev Biol *37:* 451–458.
- Bryant, P.L., J.E. Schmid, S.E. Fenton, A.R. Buckalew, B.D. Abbott (2001) Teratogenicity of 2,3,7,8-tetrachlorodibenzo-p-dioxin (TCDD) in mice lacking the expression of EGF and/or TGF-alpha. Toxicol Sci *62:* 103–114.
- Burdett, D.N., J.D. Waterfield, R.M. Shah (1988) Vertical development of the secondary palate in hamster embryos following exposure to 6-mercaptopurine. Teratology *37:* 591–597.
- Carette, M.J., M.W. Ferguson (1992) The fate of medial edge epithelial cells during palatal fusion in vitro: an analysis by DiI labelling and confocal microscopy. Development *114:* 379–388.
- Citterio, H.L., D.A. Gaillard (1994) Expression of transforming growth factor alpha (TGF alpha), epidermal growth factor receptor (EGF-R) and cell proliferation during human palatogenesis: an immunohistochemical study. Int J Dev Biol *38:* 499–505.
- Cobourne, M.T., G.M. Xavier, M. Depew, L. Hagan, J. Sealby, Z. Webster, P.T. Sharpe (2009) Sonic hedgehog signalling inhibits palatogenesis and arrests tooth development in a mouse model of the nevoid basal cell carcinoma syndrome. Dev Biol *331:* 38–49.
- Cuervo, R., L. Covarrubias (2004) Death is the major fate of medial edge epithelial cells and the cause of basal lamina degradation during palatogenesis. Development *131:* 15–24.
- Cui, X.M., Y. Chai, J. Chen, T. Yamamoto, Y. Ito, P. Bringas, C.F. Shuler (2003) TGF-beta3-dependent SMAD2 phosphorylation and inhibition of MEE proliferation during palatal fusion. Dev Dyn *227:* 387–394.
- Dixon, M.J., J. Garner, M.W. Ferguson (1991) Immunolocalization of epidermal growth factor (EGF), EGF receptor and transforming growth factor alpha (TGF alpha) during murine palatogenesis in vivo and in vitro. Anat Embryol (Berl) *184:* 83–91.
- Dudas, M., A. Nagy, N.J. Laping, A. Moustakas, V. Kaartinen (2004) TGF-beta3-induced palatal fusion is mediated by Alk-5/Smad pathway. Dev Biol *266:* 96–108.
- Ferguson, M.W. (1988) Palate development. Development *103(suppl):* 41–60.
- Fitchett, J.E., E.D. Hay (1989) Medial edge epithelium transforms to mesenchyme after embryonic palatal shelves fuse. Dev Biol *131:* 455–474.
- Fitzpatrick, D.R., F. Denhez, P. Kondaiah, R.J. Akhurst (1990) Differential expression of TGF beta isoforms in murine palatogenesis. Development *109:* 585–595.
- Gato, A., M.L. Martinez, C. Tudela, I. Alonso, J.A. Moro, M.A. Formoso, M.W. Ferguson, C. Martinez-Alvarez (2002) TGF-beta(3)-induced chondroitin sulphate proteoglycan mediates palatal shelf adhesion. Dev Biol *250:* 393–405.
- Gawel-Thompson, K.J., R.M. Greene (1989) Epidermal growth factor: modulator of murine embryonic palate mesenchymal cell proliferation, polyamine biosynthesis, and polyamine transport. J Cell Physiol *140:* 359–370.
- Gehris, A.L., M.M. Pisano, P. Nugent, R.M. Greene (1994) Regulation of TGF beta 3 gene expression in embryonic palatal tissue. In Vitro Cell Dev Biol Anim *30A:* 671–679.
- Greene, R.M., R.M. Pratt (1976) Developmental aspects of secondary palate formation. J Embryol Exp Morphol *36:* 225–245.
- Heldin, C.H., B. Westermark (1990) Signal transduction by the receptors for platelet-derived growth factor. J Cell Sci *96:* 193–196.
- Hilliard, S.A., L. Yu, S. Gu, Z. Zhang, Y.P. Chen (2005) Regional regulation of palatal growth and patterning along the anterior-posterior axis in mice. J Anat *207:* 655–667.
- Hudson, C.D., B.L. Shapiro (1973) A radioautographic study of deoxyribonucleic acid synthesis in embryonic rat palatal shelf epithelium with reference to the concept of programmed cell death. Arch Oral Biol *18:* 77–84.
- Iamaroon, A., B. Tait, V.M. Diewert (1996) Cell proliferation and expression of EGF, TGF-alpha, and EGF receptor in the developing primary palate. J Dent Res *75:* 1534–1539.

Izvolsky, K.I., D. Shoykhet, Y. Yang, Q. Yu, M.A. Nugent, W.V. Cardoso (2003) Heparan sulfate-FGF10 interactions during lung morphogenesis. Dev Biol *258:* 185–200.

Jaskoll, T., H.A. Choy, H. Chen, M. Melnick (1996) Developmental expression and CORT-regulation of TGF-beta and EGF receptor mRNA during mouse palatal morphogenesis: correlation between CORT-induced cleft palate and TGF-beta 2 mRNA expression. Teratology *54:* 34–44.

Jin, J.Z., J. Ding (2006) Analysis of cell migration, transdifferentiation and apoptosis during mouse secondary palate fusion. Development *133:* 3341–3347.

Kaartinen, V., X.M. Cui, N. Heisterkamp, J. Groffen, C.F. Shuler (1997) Transforming growth factor-beta3 regulates transdifferentiation of medial edge epithelium during palatal fusion and associated degradation of the basement membrane. Dev Dyn *209:* 255–260.

Kaartinen, V., J.W. Voncken, C. Shuler, D. Warburton, D. Bu, N. Heisterkamp, J. Groffen (1995) Abnormal lung development and cleft palate in mice lacking TGF-beta 3 indicates defects of epithelial-mesenchymal interaction. Nat Genet *11:* 415–421.

Knight, A.S., B.C. Schutte, R. Jiang, M.J. Dixon (2006) Developmental expression analysis of the mouse and chick orthologues of IRF6: the gene mutated in Van der Woude syndrome. Dev Dyn *235:* 1441–1447.

Levi, G., S. Mantero, O. Barbieri, D. Cantatore, L. Paleari, A. Beverdam, F. Genova, B. Robert, G.R. Merlo (2006) Msx1 and Dlx5 act independently in development of craniofacial skeleton, but converge on the regulation of Bmp signaling in palate formation. Mech Dev *123:* 3–16.

Liu, W., X. Sun, A. Braut, Y. Mishina, R.R. Behringer, M. Mina, J.F. Martin (2005) Distinct functions for Bmp signaling in lip and palate fusion in mice. Development *132:* 1453–1461.

Lu, H., Y. Jin, G.L. Tipoe (2000) Alteration in the expression of bone morphogenetic protein-2,3,4,5 mRNA during pathogenesis of cleft palate in BALB/c mice. Arch Oral Biol *45:* 133–140.

Martinez-Alvarez, C., M.J. Blanco, R. Perez, M.A. Rabadan, M. Aparicio, E. Resel, T. Martinez, M.A. Nieto (2004) Snail family members and cell survival in physiological and pathological cleft palates. Dev Biol *265:* 207–218.

Martinez-Alvarez, C., R. Bonelli, C. Tudela, A. Gato, J. Mena, S. O'Kane, M.W. Ferguson (2000a) Bulging medial edge epithelial cells and palatal fusion. Int J Dev Biol *44:* 331–335.

Martinez-Alvarez, C., C. Tudela, J. Perez-Miguelsanz, S. O'Kane, J. Puerta, M.W. Ferguson (2000b) Medial edge epithelial cell fate during palatal fusion. Dev Biol *220:* 343–357.

Martinez-Sanz, E., A. Del Rio, C. Barrio, J. Murillo, E. Maldonado, B. Garcillan, M. Amoros, T. Fuerte, A. Fernandez, E. Trinidad M.A., Rabadan, Y. Lopez, M.L. Martinez, C. Martinez-Alvarez (2008) Alteration of medial-edge epithelium cell adhesion in two Tgfbeta3 null mouse strains. Differentiation *76:* 417–430.

Meng, L., Z. Bian, R. Torensma, J.W. Von den Hoff (2009) Biological mechanisms in palatogenesis and cleft palate. J Dent Res *88:* 22–33.

Miettinen, P.J., J.R. Chin, L. Shum, H.C. Slavkin, C.F. Shuler, R. Derynck, Z. Werb (1999) Epidermal growth factor receptor function is necessary for normal craniofacial development and palate closure. Nat Genet *22:* 69–73.

Mori, C., N. Nakamura, Y. Okamoto, M. Osawa, K. Shiota (1994) Cytochemical identification of programmed cell death in the fusing fetal mouse palate by specific labelling of DNA fragmentation. Anat Embryol (Berl) *190:* 21–28.

Murillo, J., E. Maldonado, M.C. Barrio, A. Del Rio, Y. Lopez, E. Martinez-Sanz, I. Gonzalez, C. Martin, I. Casado, C. Martinez-Alvarez (2009) Interactions between TGF-beta1 and TGF-beta3 and their role in medial edge epithelium cell death and palatal fusion in vitro. Differentiation *77:* 209–220.

Nawshad, A., D. Medici, C.C. Liu, E.D. Hay (2007) TGFbeta3 inhibits E-cadherin gene expression in palate medial-edge epithelial cells through a Smad2-Smad4-LEF1 transcription complex. J Cell Sci *120:* 1646–1653.

Nie, X.G. (2005) Differential expression of Bmp2, Bmp4 and Bmp3 in embryonic development of mouse anterior and posterior palate. Chin Med J (Engl) *118:* 1710–1716.

Nugent, P., R.M. Greene (1998) MSX-1 gene expression and regulation in embryonic palatal tissue. In Vitro Cell Dev Biol Anim *34:* 831–835.

Nugent, P., L. Ma, R.M. Greene (1998) Differential expression and biological activity of retinoic acid-induced TGFbeta isoforms in embryonic palate mesenchymal cells. J Cell Physiol *177:* 36–46.

Pantalacci, S., J. Prochazka, A. Martin, M. Rothova, A. Lambert, L. Bernard, C. Charles, L. Viriot, R. Peterkova , V. Laudet (2008) Patterning of palatal rugae through sequential addition reveals an anterior/posterior boundary in palatal development. BMC Dev Biol *8:* 116.

Patel, D., A. Lahiji, S. Patel, M. Franklin, X. Jimenez, D.J. Hicklin, X. Kang (2007) Monoclonal antibody cetuximab binds to and down-regulates constitutively activated epidermal growth factor receptor vIII on the cell surface. Anticancer Res *27:* 3355–3366.

Pelton, R.W., B.L. Hogan, D.A. Miller, H.L. Moses (1990) Differential expression of genes encoding TGFs beta1, beta2, and beta3 during murine palate formation. Dev Biol *141:* 456–460.

Pratt, R.M., G.R. Martin (1975) Epithelial cell death and cyclic AMP increase during palatal development. Proc Natl Acad Sci USA *72:* 874–877.

Proetzel, G., S.A. Pawlowski, M.V. Wiles, M. Yin, G.P. Boivin, P.N. Howles, J. Ding, M.W. Ferguson, T. Doetschman (1995) Transforming growth factor-beta 3 is required for secondary palate fusion. Nat Genet *11:* 409–414.

Qiu, C.X., M.W. Ferguson (1995) The distribution of PDGFs and PDGF-receptors during murine secondary palate development. J Anat *186:* 17–29.

Resel, E., E. Martínez-Sanz, I. González, E. Trinidad, B. Garcillán, M. Amorós, C. Alonso-Bañuelos, B. González-Meli, E. Lagarón, J. Murillo, A. Del Río, C. Barrio, M. López, C. Martínez-Álvarez (2007) In vitro manipulation of cleft palate connective tissue: setting the bases of a proposed new treatment. J Surg Res *138:* 111–120.

Rice, R., B. Spencer-Dene, E.C. Connor, A. Gritli-Linde, A.P. McMahon, C. Dickson, I. Thesleff, D.P. Rice (2004) Disruption of Fgf10/Fgfr2b-coordinated epithelial-mesenchymal interactions causes cleft palate. J Clin Invest *113:* 1692–1700.

Sasaki, Y., S. O'Kane, J. Dixon, M.J. Dixon, M.W. Ferguson (2007) Temporal and spatial expression of Pax9 and Sonic hedgehog during development of normal mouse palates and cleft palates in TGF-beta3 null embryos. Arch Oral Biol *52:* 260–267.

Satokata, I., R. Maas (1994) Msx1 deficient mice exhibit cleft palate and abnormalities of craniofacial and tooth development. Nat Genet *6:* 348–356.

Shah, R.M., A.V. Young, B.Z. Song, D.T. Wong (1994) A novel approach to the growth analysis of hamster secondary palate by histone 3 mRNA in situ hybridization. Histol Histopathol *9:* 669–675.

Sharpe, P.M., D.M. Foreman, M.J. Carette, S.L. Schor, M.W. Ferguson (1992) The effects of transforming growth factor-beta 1 on protein production by mouse embryonic palate mesenchymal cells in the presence or absence of serum. Arch Oral Biol *37:* 39–48.

Shiota, K., S. Fujita, T. Akiyama, C. Mori (1990) Expression of the epidermal growth factor receptor in developing fetal mouse palates: an immunohistochemical study. Am J Anat *188:* 401–408.

Shuler, C.F., D.E. Halpern, Y. Guo, A.C. Sank (1992) Medial edge epithelium fate traced by cell lineage analysis during epithelial-mesenchymal transformation in vivo. Dev Biol *154:* 318–330.

Takigawa, T., K. Shiota (2004) Terminal differentiation of palatal medial edge epithelial cells in vitro is not necessarily dependent on palatal shelf contact and midline epithelial seam formation. Int J Dev Biol *48:* 307–317.

Taya, Y., S. O'Kane, M.W. Ferguson (1999) Pathogenesis of cleft palate in TGF-beta3 knockout mice. Development *126:* 3869–3879.

Tudela, C., M.A. Formoso, T. Martinez, R. Perez, M. Aparicio, C. Maestro, A. Del Rio, E. Martinez, M. Ferguson, C. Martinez-Alvarez (2002) TGF-beta3 is required for the adhesion and intercalation of medial edge epithelial cells during palate fusion. Int J Dev Biol *46:* 333–336.

Turecková, J., C. Sahlberg, T. Aberg, J.V. Ruch, I. Thesleff, R. Peterkova (1995) Comparison of expression of the msx-1, msx-2, BMP-2 and BMP-4 genes in the mouse upper diastemal and molar tooth primordia. Int J Dev Biol *39:* 459–468.

Vaziri Sani, F., K. Hallberg, B.D. Harfe, A.P. McMahon, A. Linde, A. Gritli-Linde (2005) Fate-mapping of the epithelial seam during palatal fusion rules out epithelial-mesenchymal transformation. Dev Biol *285:* 490–495.

Weston, W.M., M.B. Potchinsky, C.M. Lafferty, L. Ma, R.M. Greene (1998) Cross-talk between signaling pathways in murine embryonic palate cells: effect of TGF beta and cAMP on EGF-induced DNA synthesis. In Vitro Cell Dev Biol Anim *34:* 74–78.

Xu, X., J. Han, Y. Ito, P. Bringas Jr., M.M. Urata, Y. Chai (2006) Cell autonomous requirement for Tgfbr2 in the disappearance of medial edge epithelium during palatal fusion. Dev Biol *297:* 238–248.

Yamamoto, T., X.M. Cui, C.F. Shuler (2003) Role of ERK1/2 signaling during EGF-induced inhibition of palatal fusion. Dev Biol *260:* 512–521.

Yang, L.T., V. Kaartinen (2007) Tgfb1 expressed in the Tgfb3 locus partially rescues the cleft palate phenotype of Tgfb3 null mutants. Dev Biol *312:* 384–395.

Yu, Z., J. Lin, Y. Xiao, J. Han, X. Zhang, H. Jia, Y. Tang , Y. Li (2005) Induction of cell-cycle arrest by all-trans retinoic acid in mouse embryonic palatal mesenchymal (MEPM) cells. Toxicol Sci *83:* 349–354.

Zhang, Z., Y. Song, X. Zhao, X. Zhang, C. Fermin, Y. Chen (2002) Rescue of cleft palate in Msx1-deficient mice by transgenic Bmp4 reveals a network of BMP and Shh signaling in the regulation of mammalian palatogenesis. Development *129:* 4135–4146.